RSC Advances




ROYAL SOCIETY OF CHEMISTRY

www.rsc.org/advances

# Bilayer Interaction and Protein Kinase C-C1 Domain binding studies of Kojic Acid Esters

Rituparna Borah, Dipjyoti Talukdar, Sukhamoy Garai, Dipankar Bain and Debasis Manna*

Synthesis of kojic acid ester analogues and its lipid bilayer interaction and PKC-C1 domain binding properties has been demonstrated in this present work.

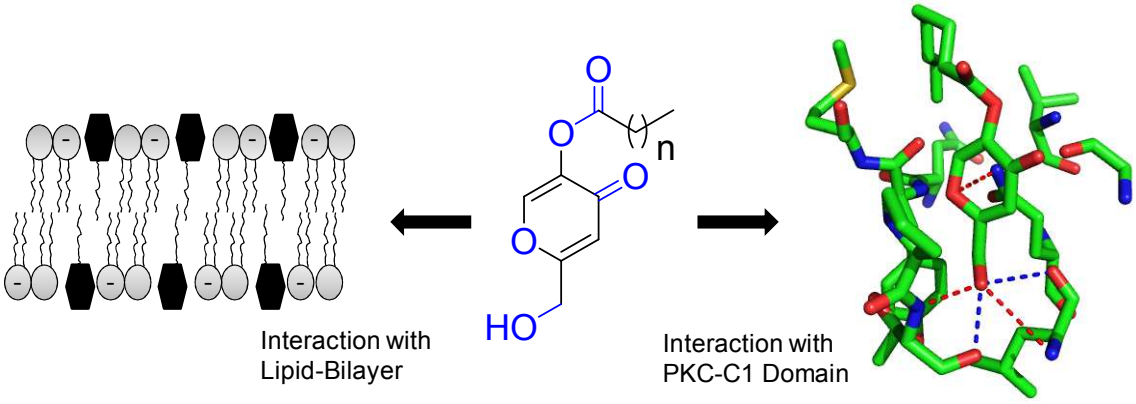

# Bilayer Interaction and Protein Kinase C-C1 Domain binding studies of Kojic Acid Esters

Rituparna Borah, Dipjyoti Talukdar, Sukhamoy Gorai, Dipankar Bain and Debasis Manna*



**ABSTRACT**

Development of protein kinase C (PKC) regulators has been considered as an attractive therapeutic strategy for the treatment of cancer and other diseases. Extensive efforts are underway to synthesize PKC regulators targeted to the DAG-responsive C1 domain. Investigation of physicochemical properties of the synthesized molecules also is essential for the development of PKC-C1 domain ligands. To develop PKC regulators, we conveniently synthesized kojic acid esters targeted to the DAG/phorbol ester binding site within the C1 domain. Physicochemical studies showed that the kojic acid esters aggregate in aqueous solution at reasonably lower concentration. The results also showed that the compounds strongly interact with the lipid bilayer and the hydrophilic part of the compound localize at the bilayer/water interface. In-vitro protein binding studies and molecular docking analysis revealed that the hydroxymethyl group, carbonyl groups and acyl chain length are important for their interaction with the C1 domain. The potent compound showed more than 10-fold stronger binding affinity for the C1 domain than DAG. In addition to the diverse application of kojic acid esters in food, cosmetic and

skin-health industries, these findings reveal that ester analogues represent an attractive group of C1- domain ligand that can be further structurally modified to improve their binding and activity.

## INTRODUCTION

The lipophilic second messenger sn-1,2-diacylglycerol (DAG) mediates a wide variety of cellular processes including cell proliferation, differentiation, malignant transformation and others.[1-3] Mammalian cells contain low concentrations of DAGs under equilibrium condition.[1, 2] Stimulation of phosphatidylinositol-specific phospholipase C (PI-PLC) enzyme by an array of G-protein-coupled receptors and receptor tyrosine kinases catalyze the hydrolysis of phosphatidylinositol-4,5 bisphosphate [PtdIns(4,5)$P_2$] to generate DAGs and inositol-1,4,5-triphosphate [(1,4,5)$IP_3$]. The DAGs activates conventional and novel protein kinase C (PKC) isoenzymes in the presence of anionic phospholipids at the plasma membranes and transmit their signal by phosphorylating target proteins. The other hydrolysis product, (1,4,5)$IP_3$ stimulates the releases of $Ca^{2+}$ from the endoplasmic reticulum (ER), which also turn on various proteins including $Ca^{2+}$-dependent PKC isoenzymes.[1-6]

The N-terminal regulatory domain of PKC proteins contains an autoinhibitory sequence and one or two membrane targeting domains (C1 and C2). Position of the pseudosubstrate sequences of the regulatory domain within/out of the catalytic site directly controls the enzyme activity.[7, 8] The reversible cellular translocation of classical PKC isoenzyme to the inner plasma membrane is initially mediated by $Ca^{2+}$ binding

through C2 domain, followed by C1 domain-DAG interactions. DAG binding to the C1 domains is generally known to activate novel PKC isoenzymes. However, a recent study also showed that protein binding to the C2 domain can also activate the PKC isoenzymes.[9] DAG binding to the C1 domain leads the folding-out of N-terminal pseudosubstrate sequence from the catalytic site, which allows access of a myriad of substrates to the catalytic site of the PKC isozymes.[10] DAGs also activates several other families of signaling proteins, e.g. RasGRPs and chimaerins, which share with PKC the C1 domain as a DAG recognition motif. PKC family of proteins plays a crucial role in the pathology of several diseases including, cancer, neurological, immunological, cardiovascular, and Alzheimer's diseases. Hence, PKC isoenzymes have been a subject of intensive research and drug development.[11-16]

The catalytic domain of PKC isoenzymes is extensively homologous with several other protein kinases in the human genome.[15] Therefore, regulation of PKC enzyme activity by targeting its C1 domain provides a more rational approach.[12, 17] A number of studies have already described that the regulatory domain of PKC isoenzymes might have independent biological functions. The C1 domains are smaller in sizes, retain conserved structure and contain only one ligand binding site. Also, the number of C1 domain containing host proteins is small. In consequence, a variety of PKC regulators directed to the C1 domain have been developed as a new class of antitumor agents.[15, 18-23] However, most of the reported high-affinity C1-domain ligands are structurally rigid and complex natural products.[3, 4, 6, 13, 17] In our continuous effort to design simple surrogates, whose structure can be easily modified to achieve higher specificity and selectivity among the

C1 domains of the PKC isoenzymes, we have selected kojic acid as a template for the current study.

Kojic acid is a secondary metabolite, generated from carbohydrate sources in an aerobic process by various fungi and bacteria, such as Aspergillus and Penicillium.[24] The derivatives of kojic acid are present in a range of natural and synthetic products with intriguing pharmacological activities. Kojic acid is one of the most meticulously studied inhibitor of tyrosinase.[25, 26] This natural pyrone and its derivatives are widely used as a food preservative for preventing enzymatic browning, cosmetic skin-whitening agent for the treatment of melasma, antioxidant, antitumor agent and radioprotective agent. Kojic acid plays a significant role in iron-overloaded diseases like anemia, due to its iron-chelating activity. Kojic acid and its derivatives also show antibiotic, anti-diabatic, anti-inflammatory, anti-proliferative and other activities.[25-28] Several attempts to improve the anticancer potential of kojic acid by introducing various chemical moieties to the compound have been already attempted by researchers. Kojic acid esters contain both hydrophobic (palmitate, oleate, stearate and others) and hydrophilic (5-hydroxy-2-hydroxymethyl-4-pyrone) groups. In spite of its significant importance, to the best of our knowledge; there is no report available on the interaction of kojic acid ester molecule with the lipid bilayer and their binding properties with the PKC isoenzymes.

In this context, the present study describes the synthesis, aggregation behavior in aqueous solution, interaction properties with the lipid bilayers, and in vitro binding properties of kojic acid esters to the C1b subdomains of PKCδ and PKCθ. The long chain kojic acid ester analogues increase the fluidity and permeability of the model membranes, which assists their binding capabilities with the PKC-C1b subdomains. The active kojic

acid ester analogues can compete with DAG binding to the C1b subdomains of PKCs. The hydroxymethyl group, pyrone ring and a suitable hydrophobic ester group of the compounds play a decisive role in recognizing the C1b subdomains of PKC isoenzymes.

## EXPERIMENTAL SECTION

**General Information:** All reagents were purchased from Sigma (St. Louis MO), SRL (Mumbai, India), Merck (Mumbai, India) and used directly without further purification. Dry solvents were obtained according to the reported procedures. Column chromatography was performed using 60—120 mesh silica gel. Reactions were monitored by thin-layer chromatography (TLC) on silica gel 60 F254 (0.25 mm). $^{1}$H NMR and $^{13}$C NMR spectra were recorded at 400 and 100 MHz, respectively using a Varian AS400 spectrometer. Coupling constants (*J* values) are reported in hertz, and chemical shifts are reported in parts per million (ppm) downfield from tetramethylsilane using residual chloroform ($\delta$ = 7.24 for $^{1}$H NMR, $\delta$ = 77.23 for $^{13}$C NMR) as an internal standard. Multiplicities are reported as follows: s (singlet), d (doublet), t (triplet), m (multiplet), and br (broadened). Mass spectra were recorded using a Waters Q-TOF Premier mass spectrometry system, and data were analyzed using the built-in software. 1,2-dipalmitoyl-sn-glycerol ($DAG_{16}$), 1,2-dioctanoyl-sn-glycerol ($DAG_8$), 1,2-dipalmitoyl-*sn*-glycero-3-phosphocholine (DPPC), 1,2-dipalmitoyl-*sn*-glycero-3-phospho-L-serine (DPPS), 1,2- dipalmitoyl-*sn*-glycero-3-phosphoethanolamine (DPPE), 1,2-dioleoyl-*sn*-glycero-3-phosphoethanolamine-N-(5-dimethylamino-1

naphthalenesulfonyl) (NBD-PE), were purchased from Avanti Polar Lipids (Alabaster, AL). Ultrapure water (Milli-Q system, Millipore, Billerica, MA) was used for the preparation of buffers.

**Synthesis of kojic acid esters:**

**General procedure for THP protection of kojic acid:** To a stirring solution of kojic acid (1 equiv) and dihydropyrane (1.2 equiv) in $CH_2Cl_2$ (10 mL), anhydrous p-toluenesulfonic acid (0.05 equiv) was added. The reaction mixture was then stirred for 1.5 hours at room temperature. After completion of the reaction (monitored by TLC), the solvent was removed under reduced pressure and the excess acid was neutralized by using 10% (w/v) solution of NaOH. The reaction mixtures was extracted with $CH_2Cl_2$ (3 × 25 mL), dried over anhydrous $Na_2SO_4$ and concentrated under reduced pressure. Column chromatography with silica gel and a gradient solvent system of ethylacetate to hexane yielded the target compound. The purification by silica gel column chromatography and a gradient solvent system of 0–20% ethyl acetate to hexanes yielded the target compound (910 mg, 57.7%).

**General procedure for esterification**: To a stirring solution of THP-protected kojic acid in $CH_2Cl_2$ (10 mL) N,N dicyclohexylcarbodiimide (1.5 equiv) and 4-dimethylaminopyridine (0.2 equiv) were added. The solution was stirred for 15 minutes and then respective fatty acids (1 equiv) were added. After the completion of reaction, the urea derivative was filtered off and washed with saturated ammonium chloride solution. The reaction mixtures was extracted with ethylacetate (3 × 15 mL), dried over anhydrous

$Na_2SO_4$ and concentrated under reduced pressure. The purification by silica gel column chromatography and a gradient solvent system of 0–20% ethyl acetate to hexanes yielded the target compound.

**General procedure for THP deprotection:** To a stirring solution of THP-protected ester (1 equiv) in $CH_2Cl_2$, p-toluenesulfonic acid (0.2 equiv) was added. The solution was stirred for 2.5 hours at room temperature. After completion of the reaction, the solvent was removed under reduced pressure. The reaction mixture was first washed with distilled water, and then pH of the solution was adjusted to 6 using $Na_2CO_3$ solution. The reaction mixtures was extracted with ethylacetate (3 × 15 mL), dried over anhydrous $Na_2SO_4$ and concentrated under reduced pressure. The purification by silica gel column chromatography and a gradient solvent system of 0–20% ethyl acetate to hexanes yielded the target compound.

**Critical aggregation concentration (CAC) measurement:** For the CAC calculation, stock solution of compound **4** and **5** were prepared in ultrapure water (with 1% ethanol) and then test solutions of desired concentration were prepared by adding the required volume of the compounds to a fixed concentration of ANS solution (4 μM). All the solutions were equilibrated for 2 hours before analysis. Changes in ANS fluorescence signal at 511 nm ($\lambda_{ex}$ = 380 nm) were measured using a Fluoromax-4.

**Measurement of aggregates formation by Dynamic Light Scattering (DLS) method:** The dynamic Light Scattering (DLS) measurement was performed to measure the hydro

dynamic diameter of the aggregates formed in aqueous solution (PBS buffer pH 7.0) using a Zetasizer Nano ZS (Malvem Instrument Lab., Malvern, U.K.) light scattering spectrometer equipped with a He–Ne laser working at 4 mW ($\lambda_0$ = 632.8 nm).[29, 30] The sample solutions were filtered off through a syringe filter (0.22 μm) and equilibrated for 10 min before performing any measurement (at least 11 runs were performed for each sample). All measurements were performed at room temperature and the scattering intensity was measured at 90° (right angle) to the incident beam.

**Liposome preparation:** Vesicles for the determination of partition coefficient and phase transition temperature were prepared according to the reported procedure. Briefly, lipids were dried out from chloroform solutions to form a thin film. The films were hydrated with phosphate-buffered saline (PBS), pH 7. The preparations were then sonicated at 50 °C for 2 minutes to prepare vesicles (final concentration 1 mM). The small unilamellar vesicles were prepared by extruding through a polycarbonate membrane (100 nm) using a handheld mini-extruder at room temperature. For labeling experiment, NpOH in PBS buffer at PH 7 was added to the solution containing vesicles. The lipid solution was incubated with NpOH solution at 55 $^0$C for 30 min with lipid/probe ratio at 100.

**Determination of partition coefficient of 1-naphthol in DPPC bilayer:** The partition coefficient of 1-naphthol (NpOH) in aqueous solution of DPPC vesicle was measured by monitoring the NpOH* emission peak as reported earlier. A series of solutions with fixed concentration of NpOH (4 μM) and varying concentrations of DPPC vesicle (0.01-0.1 mM) were prepared for the measurement. The other series of lipid solutions were also

prepared accordingly in the presence of compound **4** and **5**. Fluorescence spectra of NpOH were recorded both in SG ($30^0$ C) and LC phase ($53^0$ C) of the DPPC vesicles. The partition coefficient ($K_p$) of NpOH was calculated from the slope of the double reciprocal plot of 1/F *vs.* 1/L using the eq 1, where, $F_0$ and F represent the fluorescence intensity of NpOH* ($\lambda_{em}$ = 370 nm) in the absence or presence of DPPC liposomes, respectively.

$$\frac{1}{F} = \frac{55.6}{(K_p F_0 L)} + \frac{1}{F_0} \quad (1)$$

The membrane bound fraction ($X_L$) of NpOH was calculated using the eq 2. The used molar concentration of lipid (L) was 0.1 mM.

$$X_L = \frac{K_P L}{(55.6 + K_P L)} \quad (2)$$

**Measurement of phase transition temperature of DPPC liposomes:** For the measurement of phase transition temperature [31] of DPPC liposomes a series of test solutions were prepared with fixed concentration of labeled lipid. The $T_M$ value of DPPC liposome was determined by monitoring the fluorescence intensity of NpOH* ($\lambda_{em}$ = 370 nm) in the temperature range of $30^0$C-$55^0$C. The $T_M$ values of DPPC liposomes were also measured in the presence of varying concentrations (20-200 μM) of compound **4** and **5**.

**Extent of Membrane Localization:** The extent of localization of the ligands at the liposome interface was studied by NBD fluorescence quenching method, using PC/Ligand$_{16}$/NBD-PE liposomes (89/10/1) in 50 mM Tris buffer, pH 8.2, containing 150 mM NaCl, according to the reported procedure. The quenching reaction was initiated by adding sodium dithionite from a stock solution of 0.6 M in 50 mM Tris buffer,

pH 11 containing 150 mM NaCl, to give a final concentration of 1 mM. The change in NBD fluorescence emission intensity at 530 nm ($\lambda_{ex}$ = 469 nm) was recorded for 3 min at room temperature.

**Protein Purification:** The PKCδ and PKCθ-C1b subdomains were expressed in *E. Coli* as a GST-tagged protein, purified by glutathione sepharose column and the GST tag were removed by the thrombin treatment using methods similar to those reported earlier.[21-23]

**Fluorescence Measurements:** To calculate the binding parameters under membrane free system, ligand-induced Trp fluorescence quenching measurements were performed on a Fluoromax-4 spectrofluorometer at room temperature. The stock solutions of compounds were freshly prepared by first dissolving complexes in spectroscopic-grade dimethylsulfoxide (DMSO) and then diluted with buffer. The amount of DMSO was kept less than 3% (by volume) for each set of experiment and had no effect on any experimental results. For fluorescence titration, protein (1 μM) and varying concentration of ligands were incubated in a buffer solution (20 mM Tris, 150 mM NaCl, 50 μM $ZnSO_4$, pH 7.4) at room temperature. Protein was excited at 284 nm, and emission spectra were recorded from 300 to 550 nm. Proper background corrections were made to avoid the contribution of buffer and dilution effect. The resulting plot of Trp fluorescence as a function of ligand concentration was subject to nonlinear least-squares best-fit analysis to calculate the apparent dissociation constant for ligands ($K_D$(ML)), using eq 3, which describes binding to a single independent site.

$$(F_0 - F) = \Delta F_{\max}\left(\frac{[x]}{[x]+ K_D(\mathrm{ML})}\right) + C \qquad (3)$$

Where, F and $F_0$ represented the fluorescence intensity at 339 nm in the presence and the absence of ligand respectively. The $\Delta F_{max}$ represents the calculated maximal fluorescence change; [$x$] represents the total monomeric ligand concentration.

Fluorescence anisotropy measurements were also performed on the same fluorimeter using similar methods described earlier. All anisotropy values of the proteins in the absence or presence of compounds are the mean values of three individual determinations. The degree (*r)* of anisotropy in the tryptophan fluorescence of the proteins was calculated using eq 4, at the peak of the protein fluorescence spectrum, where $I_{VV}$ and $I_{VH}$ are the fluorescence intensities of the emitted light polarized parallel and perpendicular to the excited light, respectively, and $G = I_{VH}/I_{HH}$ is the instrumental grating factor.

$$r = \frac{(I_{VV} - GI_{VH})}{(I_{VV} + 2GI_{VH})} \quad (4)$$

Analysis of protein-to-membrane Förster resonance energy transfer (FRET) based binding assay was used to measure the binding affinity and specificity of the selected ligands under a liposomal environment. In this assay, membrane-bound C1 domain was displaced from liposomes (PC/PE/dPE/Ligand (75/15/5/5)) by the addition of the $DAG_8$. The vesicles composed of PC/PE/PS/dPE (60/15/20/5) and PC/PE/PS/dPE/Ligand (55/15/20/5/5) were used as control and for ligands, respectively. The stock solution of $DAG_8$ was titrated into the sample containing C1 domain (1 μM) and excess liposome (100 μM total lipid) in a buffer solution (20 mM Tris, 150 mM NaCl, 50 μM $ZnSO_4$, pH 7.4) at room temperature. The competitive displacement of protein from the membrane was quantitated using protein-to-membrane FRET signal ($\lambda_{ex}$ = 280 nm and $\lambda_{em}$ = 505 nm). Control experiments were performed to measure the dilution effect under similar

experimental condition and the increasing background emission arising from direct dPE excitation. Protein-to-membrane FRET signal values as a function of $DAG_8$ concentration were subjected to nonlinear least-squares-fit analysis using eq 5 to calculate apparent equilibrium inhibition constants ($K_I(DAG_8)_{app}$) for $DAG_8$.[21] Where, $[x]$ represents the total $DAG_8$ concentration and $\Delta F_{max}$ represents the calculated maximal fluorescence change.

$$F = \Delta F_{\max}\left(1 - \frac{[x]}{[x] + K_I(\mathrm{DAG_8})_{\mathrm{app}}}\right) + C \qquad (5)$$

The equilibrium dissociation constant ($K_D(L)$) for the binding of the C1 domains to the ligand-associated liposomes was calculated from eq 6, using $K_D(ML)$ and $K_I(DAG_8)_{app}$ values. Where, $[L]_{free}$ is the free ligand concentration (2.63 ± 0.04 μM). During calculation, the ligand concentration in the liposome interior was ignored, because of their inaccessibility for the protein. Thus, the protein accesses about half of lipids in the liposomes. The ligand concentration was used excess relative to the protein. The free ligand concentration was calculated by assuming that most of the protein would bind to the liposome and equimolar amount of ligand can be subtracted from the accessible ligand.

$$K_I(DAG_8)_{app} = K_D(ML)\left(1 + \frac{[L]_{free}}{K_D(L)}\right) \qquad (6)$$

**Surface Plasmon Resonance Analysis:** All surface plasmon resonance (SPR) measurements were performed (at 25 °C, flow rate of 30 μL/min) using a lipid-coated L1 sensorchip in the Biacore X100 (GE Healthcare) system as described earlier.[32-34] The vesicles composed of PC/PE/PS (60/20/20) and PC/PE/PS/Ligand (55/20/20/5) was used as control and active surface, respectively.

## RESULT AND DISCUSSION

### Synthesis of Kojic Acid Esters:

Comprehensive analysis of the crystal structure of PKCδ-C1b in complex with phorbol-13-*O*-acetate reveals that, hydroxyl and carbonyl functional groups of the phorbol ester are primarily responsible for its efficient interaction with the C1 domain.[35] The structural analysis also indicate that ligand binding site of the C1 domain is hydrophobic in nature, thus C1 domain interacts with the ligands through the backbone amine and carbonyl groups. Several studies also showed that hydrophobicity of the ligands plays an important role in C1 domain binding. The hydrophobic part of the ligands is reported to interact with the hydrophobic amino acids present surrounding the C1 domain binding site and hydrophobic moiety of the lipid bilayer.[35, 36] We have recently demonstrated that a hydroxymethyl group and ester group with hydrophobic side chain are needed for efficient binding of protocatechualdehyde derivatives with the PKC-C1 domain.

For further understanding of these structural requirements of the C1 domain ligands and development of PKC regulator, we used biologically active kojic acid derivatives for the current study. The kojic acid esters contain the required phorbol ester pharmacophores for the C1 domain binding. Kojic acid contains one primary, one secondary hydroxyl groups along with one pyrone ring. The secondary hydroxyl groups provide access to incorporate different fatty acids. The carbonyl of the pyrone ring present at the *meta*- position of the hydroxymethyl group and oxygen atom of the pyrone ring provides additional hydrogen bonding sites for the C1 domain backbone. The hydrophobic interactions are difficult to model. Thus, we synthesized a series of kojic

acid esters with different chain length to study the impact of side chains on the binding affinity. We synthesized ester derivatives of kojic acid (of secondary hydroxyl group) using commercially available kojic acid as the starting material (Scheme 1). The compound with acyl chain length of C8, C12, C15, and C18 were synthesized to study the impact of alkyl chain length on the binding affinity. It is reported that DAGs with unsaturated hydrophobic 'tail', generated by PI-PLC are more potent in PKC activation than the saturated DAGs produced by other cellular pathways.[37, 38] We prepared compound **5** with oleic acid to study the impact of unsaturated hydrophobic 'tail' in protein binding and interaction with lipid bilayers.

Molecular docking analysis revealed that the kojic acid ester analogues are anchored to the DAG/phorbol ester binding site of the PKCδ-C1 domain (Figure 1). The model structure showed that hydroxymethyl group is hydrogen-bonded to the backbone carbonyls of Thr-242 and Lue-251 and amide protons of Thr-242 and Leu-251. The oxygen atom of the pyrone ring was hydrogen-bonded with the Gln-257. The other carbonyl groups might be involved in interaction with the anionic lipid head groups, including phosphatidylserine and others for an activation at the cellular membranes.[17] The model structure showed that there is no interaction between kojic acid ester and backbone amide proton of Gly-253 residue. A similar mode of interactions of kojic acid ester with PKCθ-C1b was observed.

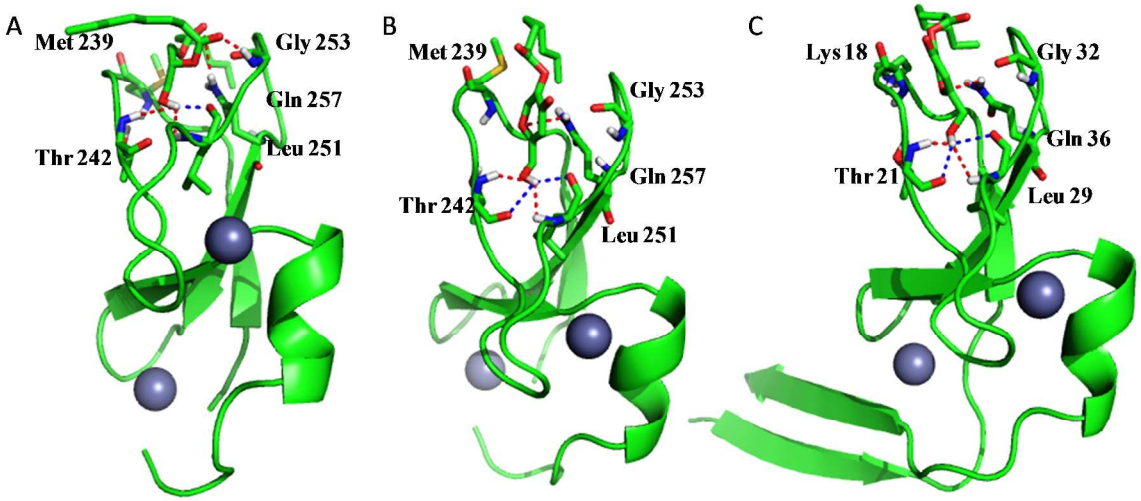


**Figure 1:** Structures of ligand bound PKCδ- and PKCθ-C1b subdomains. (A) Modeled structure of $DAG_8$ docked into PKCδ-C1b (1PTR); (B) modeled structure of **1** docked into PKCδ-C1b; (C) modeled structure of **1** docked into PKCθ-C1b (4FKD). The modeled structures were generated using the Molegro Virtual Docker, version 4.3.0. The oxygen atoms and nitrogen atoms are shown in red and blue, respectively. The dotted line indicates possible hydrogen bonds.

Kojic acid ester analogues 1-5 were synthesized from kojic acid in two steps (Scheme 1). First the primary hydroxyl group was protected with THP ether in the presence of p-toluenesulfonic acid. THP protection of primary alcohol in the presence of secondary alcohol was performed before esterification to synthesize hydroxymethyl group containing kojic acid esters only. The secondary alcohol was then esterified using the standard N,N′-dicyclohexylcarbodiimide (DCC)mediated coupling reaction with octanoic acid, dodecanic acid, palmitic acid, stearic acid and oleic acid to produce THP protected ester analogues. Subsequent removal of THP group in the presence of p-

toluenesulfonic acid provided the target kojic acid ester analogues 1-5. The selective formations of these compounds were characterized by NMR and mass spectral analyses.

**Scheme 1. Synthesis route to kojic acid esters**

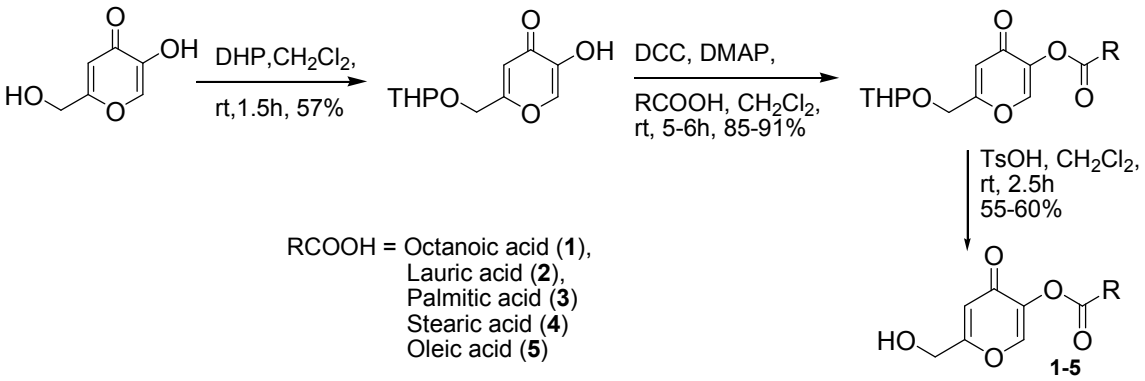


**Aggregation studies of kojic acid esters—** We first investigated the behavior of kojic acid esters in aqueous solution by measuring the fluorescence properties of 8-anilino-1-naphthalenesulfonic acid (ANS).[39, 40] The ANS have been widely used as a polarity indicator, because of its intramolecular charge transfer property. We measured the critical aggregation concentration (CAC), an analogy to illustrate critical micelle concentrations for surfactants using ANS in the presence of kojic acid esters in aqueous solution. Concentration dependent aggregation of kojic acid esters and simultaneous incorporation of ANS molecules to its hydrophobic core is reflected by the increase in fluorescence intensity and a blue shift of the ANS emission maximum. Increase in compound concentrations from 0-200 μM resulted in a blue shift of ANS emission maxima from 525 to 480 nm, supporting a continuous decrease in polarity of the medium. The plot of fluorescence intensity maximum with compound concentration suggests that around/above 50, μM, kojic acid esters **4** and **5** start aggregating (Figure 2). The

measured CAC of the compound **4** and **5** were 67 and 51 μM, respectively. These compounds with hydrophobic (palmitate and oleate) and hydrophilic (2-(hydroxymethyl)-4H-pyran-4-one) groups are expected to form aggregation in aqueous solution. However, bilayer, micelles or vesicles of kojic acid esters may not be shaped because of its high hydrophobicity and critical packing parameter (CPP).[41] We presume that, these amphiphilic molecules aggregates with irregular shapes, primarily because of the hydrophobic interaction. Due to the presence of unsaturated oleic acid, compound **5** has higher hydrophobicity than compound **4**.This allows compound **5** to aggregate at lower concentration in aqueous solution. The CAC values of these amphiphilic molecules are essential in understanding their interaction with lipid bilayer and PKC-C1 domain under monomeric form in aqueous solution. We also performed dynamic Light Scattering (DLS) measurement to confirm aggregate formation of the compounds **4** and **5** in aqueous solution (Figure S1). The results showed a monomodal (PDI = 0.423 and 1.00) size distribution around a mean hydrodynamic diameter ($d_h$) of 1000–1100 and 500-600 nm in case of compound **4** (120 μM) and **5** (150 μM) in aqueous solution (PBS buffer pH 7.0), respectively. This indicates that the compounds form large aggregates, with relatively narrow size distribution.

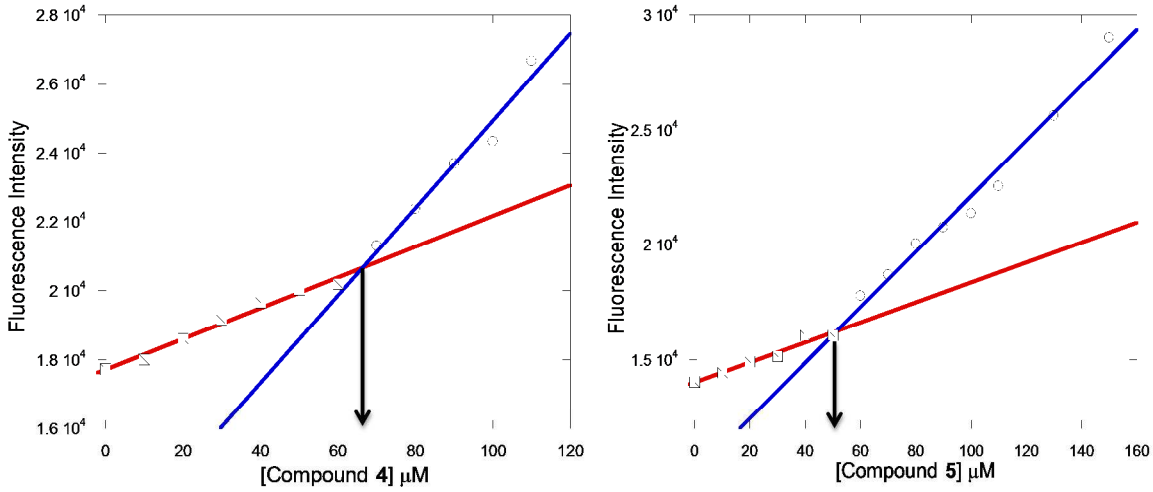


**Figure 2.** Measurement of critical aggregation concentration of compound **4** and **5** in aqueous solution. Plot of ANS fluorescence intensity against different concentration of compound (A) **4** and (B) **5**. [ANS] = 4 μM, $\lambda_{ex}$ =380 nm.

**Interaction with Lipid Bilayers:**

The effects of drug or drug-like molecules on the structure of the lipid bilayer play an important role in understanding their pathological processes. Cellular membrane properties including fluidity, permeability, surface potential and others get affected by the distribution of drug or drug-like molecules. Fluidity of the lipid bilayer and loose spacing in the polar headgroup region plays a significant role on the PKC kinase activities. Ability of the PKC-active compounds to localize at the membrane-water interface is directly linked with its C1 domain binding properties. The PKC isoenzymes get activated at the membrane interface primarily due to their interaction with the membrane localized lipophilic second messenger DAGs. The C1 domains are peripheral proteins. Therefore, the C1-domain ligands would be expected to interact significantly with the lipid bilayer and alter membrane fluidity, permeability, phase transition and others. In this regard, the

effects of kojic acid esters with the liposomes were studied by investigating their effect on permeability and phase transition of lipid bilayer and extent of membrane localization patterns.

**Effect of kojic acid esters on membrane permeability—** Recent studies showed that excited-state proton transfer (ESPT) of 1-naphthol (NpOH) is affected with the change in lipid bilayer organization.[42, 43] The change in microenvironment of the medium was investigated by using the fluorescence properties of NpOH. NpOH exists as neutral form in nonpolar media and anionic form in aqueous media. The ratio of fluorescence intensities of anionic form ($\lambda_{em}$ = 470 nm) to neutral form ($\lambda_{em}$ = 370 nm) is sensitive to the microenvironment of NpOH.[39, 44] Under liposomal environment, the origin of the NpOH* emission is due to the membrane-bound fraction of NpOH while the $NpO^-$* emission is contributed by the presence of NpOH in the semi-polar membrane interface region and unpartitioned NpOH present in water. Dipalmitoylphosphatidylcholine (DPPC) liposomes were used as a model lipid bilayer due to its high abundance in biological membranes. The plasma membrane also contains several other lipids. However, it would be difficult to monitor membrane permeability and other bilayer properties using such complex lipid compositions.

The partition coefficient ($K_p$) values of NpOH provide information regarding membrane permeability of the DPPC bilayer in the absence/presence of kojic acid esters. Membrane permeability of NpOH which increases with the increase in $K_p$ values is altered by the degree of unsaturation and chain length of the fatty acid present within the membrane active compounds.[39, 43] The changes in $K_p$ values were measured by

monitoring the changes in NpOH* fluorescence intensity. We used compound **4** and **5** with the same chain-length for this study as it would reveal the effect of saturation *vs.* unsaturation on the membrane permeability of the DPPC lipid bilayer. Figure 3A shows the double reciprocal plot of NpOH* fluorescence intensity *vs.* DPPC liposome concentration in the absence of compounds at different temperatures. Figure 3B and 3C represent the double reciprocal plot in the presence of different concentrations of compounds in the SG and LC phases of DPPC SUVs, respectively.

The $K_p$ values and mole fraction of NpOH in DPPC liposomes were calculated at different temperatures depending on DPPC lipid phases (Table 1). The results clearly showed that partitioning of NpOH is significantly higher at the phase transition temperature [31], where the permeability of the lipid bilayer membrane is expected to be higher because of the coexistence of solid and liquid domains. The results also showed that the $K_p$ value is lower in SG phase than LC phase. This could be due to the higher fluidity (higher permeability) of the lipid bilayer in the LC phase. The change in $K_p$ values are in good correlation with the change in membrane fluidity. The $K_p$ values of NpOH in the presence of both the compounds **4** and **5** enhanced with the increase in compound concentrations for both phases of the liposomes. Calculated mole fraction of NpOH partitioning into the lipid bilayer also increased in both phases of the liposomes. This clearly indicates that these compounds enhance DPPC membrane permeability and fluidity. However for compound **4**, the increase in $K_p$ value with an increase in concentration is less than that of the compound **5,** which point out that the presence of unsaturation in acyl chain increases the permeability of the lipid bilayer. In absence on DPPC liposomes, there is no NpOH* emission peak with varying concentration of the

compounds. This indicates that the compounds have no direct interactions with the NpOH molecules. Presence of kojic acid esters in the lipid bilayer might alter the packing of the polar headgroup of the DPPC molecules. The NpOH* fluorescence intensity decreases with the increase in compound concentrations (Figure S2). This could be either due to the higher membrane permeability of NpOH in the presence of compounds or could be due to the presence of water molecule within the lipid bilayer.[45] The results suggest that the amphiphilic nature of the compounds enhances its interaction with the lipid bilayer membrane with an increase in concentration.

**Table 1. Partition coefficient and mole fractions of 1-naphthol within the DPPC vesicle in the absence/presence of compound 4 and 5.**

| Liposomes | Partition coefficient ($K_p$) and mole fractions of NpOH | | |
|---|---|---|---|
| | 30 $^0$C; SG phase | 41 $^0$C; at $T_M$ | 53 $^0$C; LC phase |
| DPPC only | $0.13 \pm 0.21 \times 10^6$; $20.49 \pm 2$ % | $3.65 \pm 0.32 \times 10^5$; $40.56 \pm 1$ % | $0.14 \pm 0.19 \times 10^6$ ; $21.23 \pm 2$ % |
| DPPC + **4** (50 μM ) | $1.38 \pm 0.26 \times 10^6$; $72.05 \pm 1$ % | | $1.99 \pm 0.06 \times 10^6$; $78.79 \pm 2$ % |
| DPPC + **4** (100 μM ) | $2.10 \pm 0.19 \times 10^6$; $79.71 \pm 1$% | | $2.11 \pm 0.13 \times 10^6$; $79.82 \pm 1$% |
| DPPC + **5** (50 μM ) | $2.41 \pm 0.11 \times 10^6$; $81.86 \pm 1$ % | | $2.67 \pm 0.19 \times 10^6$; $83.34 \pm 1$% |
| DPPC + **5** (100 μM ) | $4.13 \pm 0.14 \times 10^6$; $88.53 \pm 1$% | | $8.13 \pm 0.21 \times 10^6$; $93.83 \pm 1$% |

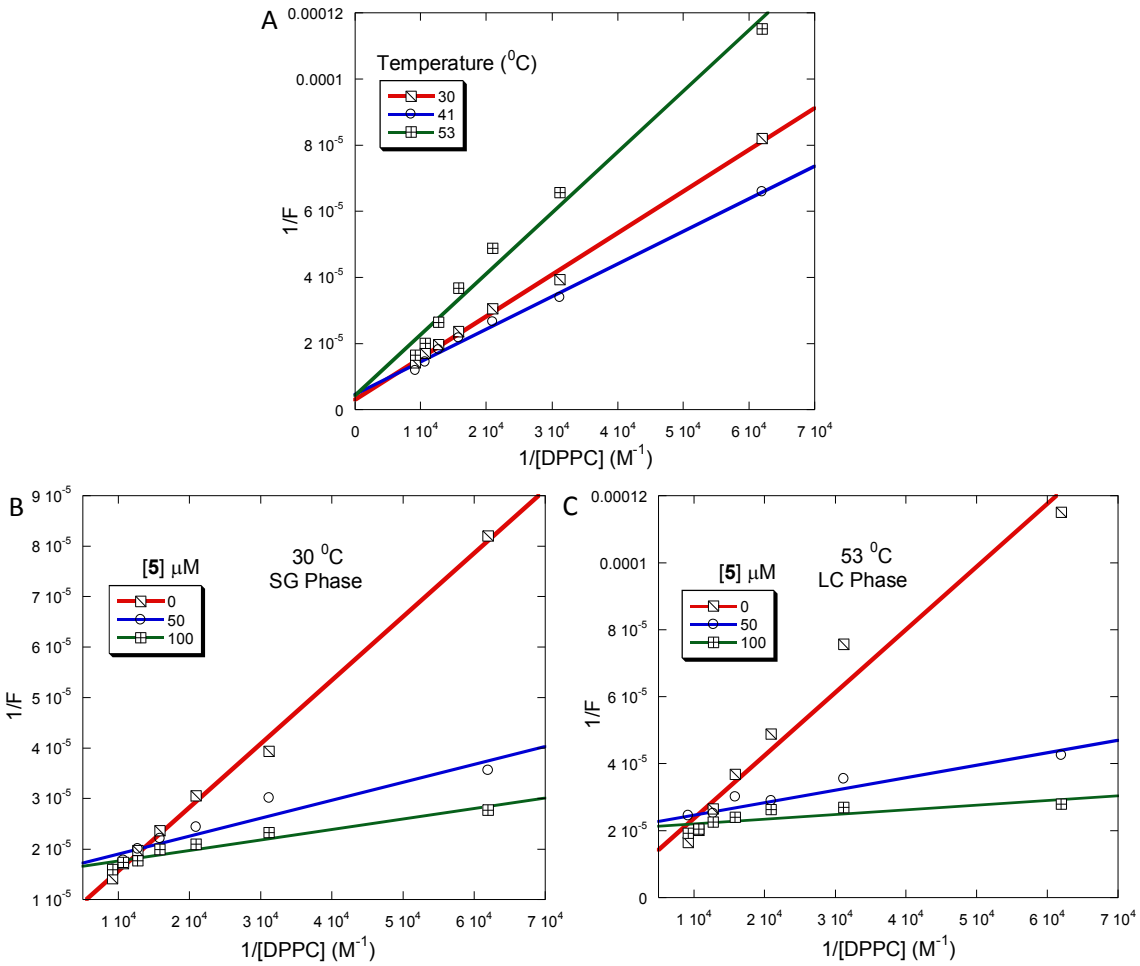


**Figure 3.** Double reciprocal plot of NpOH* fluorescence intensity *vs.* DPPC concentrations in the (A) absence of kojic acid esters, and in the presence of different concentrations of kojic acid esters in (B) SG (30 $^0$C) and (C) LC (53 $^0$C) phases; $\lambda_{ex}$ = 290 nm, $\lambda_{em}$ = 370 nm, [1-naphthol] = 4µM

**Extent of membrane localization—** The partition coefficient values of NpOH clearly showed that the kojic acid esters strongly interact with the lipid bilayer. The change in NpOH* fluorescence intensity with the increase in compound concentration also suggest that the compounds altered the packing of the DPPC headgroups. The hydrophilic part of

the amphiphilic kojic acid ester analogues are expected to be positioned near the bilayer/water interfacial region. However, the extent of localization of the pharmacophore containing hydrophilic part at the bilayer/water interface is very important for their C1 domain binding ability under liposomal environment. In this regard, we performed NBD fluorescence quenching experiments using DPPC/Ligand/NBD-PE liposomes. The NBD probe is embedded close to the bilayer/water interface, providing a useful marker for surface interactions of membrane-active C1 domain ligands.[20, 22, 23] Sodium dithionite induced NBD fluorescence quenching provided a measure of membrane localization of the ligands. Figure 4 reveals that ligand associated fluorescent liposomes showed significant changes in the rate of dithionite-induced fluorescence quenching of the bilayer-embedded probe. The ligands showed slower quenching rates than the control liposomes (without any ligands). The results indicate that the NBD probe became more 'shielded' from the soluble dithionite quencher, due to the presence of kojic acid ester analogues in the liposomes. The results also imply that hydrophilic part of these ligands are more localized at the liposome surface compared to $DAG_{16}$. Therefore, the kojic acid ester analogues are accessible for the protein binding, under liposome environment. Figure 4 indicates different degrees of localization and perturbation of the bilayer headgroup region by the kojic acid ester analogues. To further investigate the interactions of compounds with lipid bilayers and their effects upon the bilayer properties, we measured the effect of compounds on the phase transition temperature of lipid bilayer.

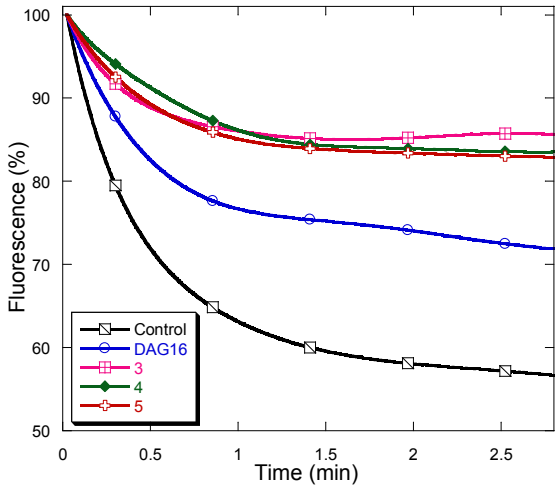


**Figure 4:** Fluorescence quenching of NBD-PE embedded in PC/Ligand$_{16}$/NBD-PE (89:10:1) liposomes. Sodium dithionite = 0.6 μM. Control: no ligand.

**Effect of kojic acid esters on the phase transition temperature of lipid bilayer—** It is well documented that the phase transition temperature of the bilayer depends on lipid compositions. The bilayer organization is also affected by nature and chain length of fatty acid, and the headgroup of the lipids.[46-48] To further probe the interaction of membrane active kojic acid esters with lipid bilayers and their effect on the fluidity of the bilayer, we measured $T_M$ values of DPPC bilayers in the absence/ presence of kojic acid esters. We used compound **4** and **5** for this study as it would also reveal the effect of saturation *vs.* unsaturation on the $T_M$ value of the DPPC lipid bilayer. The DPPC was used as a model lipid for bilayer formation. However, addition of other lipids would complicate the system.

NpOH was successfully used to study the thermotropic phase behavior of the lipid bilayer by monitoring the changes in fluorescence intensity of NpOH*. The solid gel (SG) phase of the lipid bilayer is tightly packed and has less capacity to accommodate the

probe resulting low fluorescence intensity of NpOH*. Coexistence of SG and liquid crystalline (LC) phase at the transition temperature makes the bilayer less resistant allowing local maximum in the fluorescence intensity of NpOH*. However, this fluorescence intensity gradually decreases as the region of disorder and the permeability decrease at LC phase. This temperature dependent variation of NpOH* fluorescence intensity is in accordance with the measured partition coefficient of NpOH with temperature. Therefore, we monitored the NpOH* fluorescence intensity change to measure the $T_M$ values. The variation in NpOH* fluorescence intensity with temperature demonstrates that phase transition of only DPPC lipid bilayer occurs at 41 $^0$C (Figure 5 and S2). The $T_M$ value of DPPC bilayer is in good correlation with the reported value measured by differential scanning calorimetry (DSC).[49] The results showed that the $T_M$ values of DPPC bilayer decreases from 41 $^0$C to 40 $^0$C and 39 $^0$C in the presence of compound **4** and **5**, respectively. The nature of thermotropic phase behavior also showed that the DPPC bilayer organization remains intact under these experimental conditions (Figure 5 and S3). The decrease in the $T_M$ value of the DPPC bilayer in the presence of both compounds can be attributed to the decrease in the van der Waal's interactions between hydrophobic 'tails' and alteration of lipid packing by fluidizing the region. Compound **5** with unsaturated acyl chain showed lower $T_M$ value than the compound **4**, which could be due to the increase in the fluidity of the bilayer as observed in partition coefficient measurements. The smaller change in $T_M$ values are in accordance with the NBD fluorescence quenching data, which indicate the prevalent bilayer-surface interactions of compound **4** and **5**. The localization of the headgroup of the kojic acid

esters hardly affects thermotropic phase behavior of the lipid bilayers; it primarily depends upon the 'tails' of the compounds.

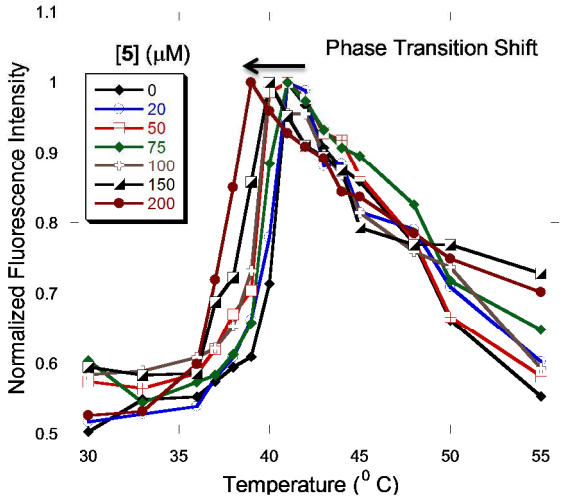


**Figure 5**. Effect of compound **5** on the phase transition temperature of DPPC vesicle. Change in NpOH* fluorescence intensity with the increase in compound **5** concentration at different temperatures in DPPC vesicles. $\lambda_{ex}$ = 290 nm, $\lambda_{em}$ = 370 nm, [DPPC] = 0.2 mM, [1-napthol] = 4 μM.

**Protein Binding Studies:**

The DAG-responsive C1 domain of classical and novel PKC isoenzymes is duplicated into a tandem C1 domain consisting of C1a and C1b subdomains. We have used the C1b subdomains of PKCδ and PKCθ proteins to measure the in vitro binding properties of the kojic acid ester analogues. These C1b subdomains are reported to have sufficiently strong DAG binding affinities and easy to obtain in soluble form from bacterial cells.[22, 50] The PKCδ- and PKCθ-C1b subdomains contains single tryptophan (Trp-252 in delta, Trp-31 in theta) and tyrosine residues (Tyr-236 and Tyr-238 in delta, Tyr-15 and Tyr-17 in

theta), respectively, which account for their intrinsic fluorescence. The protein binding properties of the kojic acid esters were measured by Trp-fluorescence quenching methods, steady-state fluorescence anisotropy and Förster resonance energy transfer (FRET) based competitive binding assay.[21-23]

**Interaction with soluble ligands—** Intrinsic fluorescence is widely used as a tool to detect the change in protein confirmation or microenvironment caused by the ligand binding. It is important to note that these C1b subdomains contain single Trp residue close to the DAG binding pocket. Figure S4 shows a representative plot of Trp-fluorescence quenching data for PKCθ-C1b subdomain in the presence of ligands. Compounds **1**–**5** quenched the Trp fluorescence (340 nm) in a concentration dependent manner, and a plateau was reached at around 15–20 μM (Figure 6 and S5). The ligand concentrations used in monomeric binding measurements were well below their CAC values of the kojic acid esters of long chain fatty acids. This clearly indicates that the compounds were in monomeric form under the experimental conditions. The measured binding affinities revealed that kojic acid esters with different chain length strongly interact with the C1b subdomains of PKCδ and PKCθ proteins. The compound **3** showed the highest affinity and other compounds have comparable binding affinities for both the proteins. The ligand **3** shows more than 10 and 13-fold stronger binding affinity than $DAG_{16}$ for PKCδ-C1b and PKCθ-C1b subdomain, respectively (Table 2). Whereas ligand **5** with unsaturated fatty acid showed more than 12 and 10-fold stronger binding affinity than $DAG_{16}$ for PKCδ-C1b and PKCθ-C1b subdomain, respectively. However,

C1b subdomains binding of the compounds in monomeric form do not show clear PKC-isoform specificity.

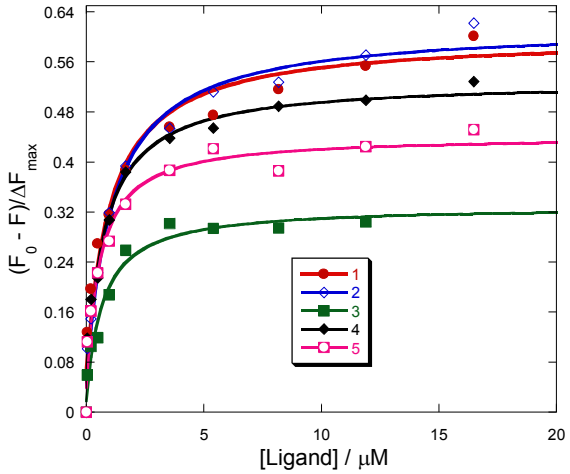


**Figure 6.** Binding of ligands with PKCδ-C1b. Representative plot of fluorescence intensity of PKCδ-C1b (1 μM) in buffer (20 mM Tris, 160 mM NaCl, 50 μM $ZnSO_4$, pH 7.4) in the presence of varying concentration of **1-5**, where F and $F_0$ are fluorescence intensity in the presence and absence of the ligands, respectively. The solid lines are nonlinear least squares best fit curves.

The molecular model structures of compound-bound protein showed that there were three hydrogen bonds between DAG and PKCδ-C1b; whereas compound **1** showed five hydrogen bonds with PKCδ-C1b. It is important to note that there was no hydrogen bond between ligand and Gly-253 of the molecular models of PKCδ-C1b, an important interaction site for ligand binding to the C1 domain. This however does not exclude the prospect of water mediated hydrogen bond formation between kojic acid ester and Gly-253 (for PKCδ-C1) or Gly-32 (for PKCθ-C1b), which was not considered during the

molecular docking analysis. This clearly indicates that measured binding parameters and docking scores obtained from the models do not always agree. This dissimilarity indicates that both protein and ligand can experience conformational alterations under experimental circumstances to produce strong interactions. Therefore, both hydroxymethyl, carbonyls (of pyrone ring and acyl group) of the kojic acid esters are important for their interaction with the PKC-C1 domains. We hypothesize that the higher binding affinity of the compounds than DAG could be due to their structural rigidity, which reduce the number of possible rotameric forms of the compounds. We also presume that one of the rigid rotamers would mimic the definite conformation of physiologically active DAG. The stronger binding of compounds to PKC-C1 domain than DAG apparently governed by the structural constrains to reduce the entropic loss due to binding.

The binding parameters also indicate that like other C1 domain ligands, some of the compounds show similar pattern of dependence on the hydrophobicity for C1 domain binding. The hydrophobic residues surrounding the binding site of the C1 domain also interact with the hydrophobic side chains of the ligands. But there is no direct relation between hydrophobicity of these compounds and their C1 domain binding affinities. For compound **1** (XLOGP3 = 2.33) and **2** (XLOGP3 = 4.11) although there is a distinct difference in hydrophobicity, the difference in binding affinity is very small and protein binding affinity for compound **2** is lower than compound **1**. Compound **3** with palmitic acid showed highest binding affinity of 0.46 μM and even higher than the compound **5** with oleic acid (unsaturated fatty acid). For kojic acid esters the difference in binding affinity is very small for both the proteins (Table 2). This could be due to the ligand

binding orientations within the binding pocket or acyl chain specificity, which was already observed for PKC-C1 domains.[51] The overall high binding affinities of the compounds are probably associated because of the hydroxymethyl and carbonyl groups. Thus, both the binding affinity values of the compounds highlight the importance of ligand hydrophobicity and binding orientation, in a manner similar to those reported for C1-domain ligands.[12, 17, 22, 52]

**Table 2. $K_D$ (ML) values for the binding of ligands with the PKCδ-C1b and PKCθ-C1b proteins[a] at room temperature.**

| Compound | $K_D$ (ML) (μM) | |
|---|---|---|
| | PKCδ-C1b | PKCθ-C1b |
| $DAG_8$ | 12.41 ± 0.59 | 6.74 ± 0.54 |
| $DAG_{16}$ | 7.04 ± 0.43 | 6.35 ± 0.37 |
| **1** | 1.04 ± 0.08 | 0.91 ± 0.06 |
| **2** | 1.09 ± 0.12 | 0.79 ± 0.09 |
| **3** | 0.69 ± 0.02 | 0.46 ± 0.01 |
| **4** | 0.77 ± 0.12 | 1.13 ± 0.03 |
| **5** | 0.57 ± 0.04 | 0.61 ± 0.05 |

[a)] Protein, 1 μM in buffer (20 mM Tris, 160 mM NaCl, 50 μM $ZnSO_4$, pH 7.4) Values represent the mean ± S.D. from triplicate measurements.

We also performed steady-state fluorescence anisotropy measurements to gain more information about ligand-protein interaction. The anisotropy values were averaged over an integration time of 10 s and a maximum number of five measurements were performed for each set of experiments. All anisotropy values of proteins in the presence of ligand are the mean values of three individual determinations. The increase in anisotropy values of the proteins in the presence of the ligands support their ligand binding. The degree of anisotropy of pure PKCδ-C1b protein increases from 0.0439 in buffer to 0.0874 upon interaction with 10-fold excesses of ligands 5 (Table S1). Similar

increases in anisotropy values were observed for the proteins in the presence of DAGs and other compounds. Although the changes in anisotropy values were different for the compounds, this experiment still suggests that the presence of the compounds increases the rigidity of the surrounding environment of the protein in a manner similar to that of DAGs.

**Interaction with ligand-associated liposomes—** Peripheral proteins like PKCs are reported to interact with the cellular membranes through their lipid-binding C1 and C2 domains.[1, 5, 7, 38] The PKC-C1 domains have both a membranes binding surface and a lipid-binding groove. The C1 domains interact with DAGs or ligands localized at the cellular membrane through its lipid-binding groove.[2, 5, 38] Therefore, to understand the C1 domain binding properties of the kojic acid esters under membrane environment, we used protein to membrane FRET-based assay. The Trp residue of the PKC-C1b subdomains serve as the FRET donor, and a low density of membrane-embedded, dansyl-PE (dPE) lipid serve as the acceptors. For the competitive binding assay active vesicles composed of PC/PE/PS/dPE (60/15/20/5) were used. PE lipid was added to improve the stability of the vesicles. PS is known induce the DAG dependent membrane binding of the C1 domain, hence it was also incorporated into the vesicles. $DAG_8$ was titrated into the solution containing C1b-subdomain-bound liposomes. The decrease in the protein-to-membrane FRET signal (Figure S6) was examined to quantitatively measure the displacement of protein from the bilayer surface to the bulk solution, and apparent inhibitory constant [$K_I(DAG_8)_{app}$] calculation. Figure 7A represents $DAG_8$ promoted competitive displacement of PKCδ-C1b subdomain from ligand associated liposomes

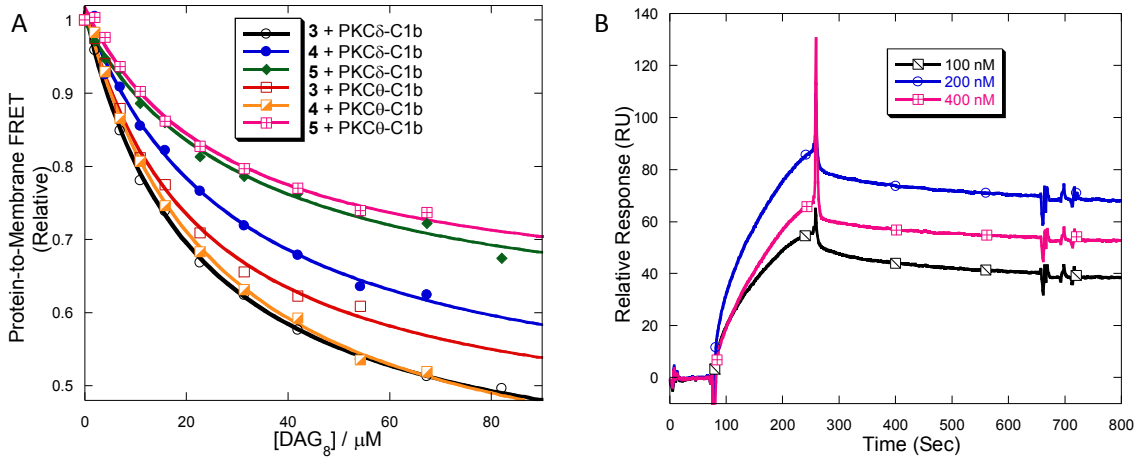


**Figure 7.** Binding isotherms under liposomal environment. (A) Competitive displacement assay for the PKCδ- and PKCθ-C1b subdomain (1 μM) bound to liposome containing ligands **3**-**5**. The bound complex was titrated with the $DAG_8$. (B) Kinetics of membrane binding of PKCδ-C1b subdomain with compound **5** containing liposomes. All sensorgrams were collected using the L1-sensor chip coated with PC/PE/PS and PC/PE/PS/**5** vesicles as reference and active surface, respectively. Flow rate was kept at 30 μl/min.

(PC/PE/dPE/Ligand). The values of $K_I(DAG_8)_{app}$ depend on ligand concentration and the background lipid composition in the liposomes as well as the affinities of the C1b subdomains for ligands. These binding parameters showed that the kojic acid esters interact with the C1b subdomains under membrane environment. This competitive binding assay confirmed that the compounds interact with the PKC-C1b subdomains through its DAG/phorbol ester binding site. The results also showed that higher concentration of $DAG_8$ was required for the displacement of PKCθ-C1b protein from the ligand associated liposomes. Finally, the equilibrium dissociation constant ($K_D$(L)) for the PKC-C1b subdomains binding to the liposome-associated targeted ligand was calculated

using equation 4.[22, 50] Comparison of the equilibrium dissociation constant also revealed that C1b-subdomains have higher binding affinity for the ligand associated liposomes (Table 3). We also measured the interaction of compounds with PKCδ-C1b subdomain using surface plasmon resonance (SPR) analysis. The measured binding parameters also demonstrated that compound **5** strongly interact with the PKCδ-C1b subdomain, under the experimental conditions ($K_D$ = 5.85 ± 0.15 nM). The SPR sensorgrams showed that the PKCδ-C1b subdomain binding to these compounds is mostly directed by a slow dissociation from the membrane interface, a distinctive property of the PKC-C1 domains (Figure 7B).[34] It is also important to mention that the protein binding affinities of the

**Table 3: Equilibrium parameters for PKCδ-C1b and PKCθ-C1b protein[a] binding to the ligand associated liposomes[b] at room temperature.**

| Compound | $K_I(DAG_8)_{app}$ (μM) | | $K_D$(L) (nM) | |
|---|---|---|---|---|
| | PKCδ-C1b | PKCθ-C1b | PKCδ-C1b | PKCθ-C1b |
| **3** | 21.73 ± 2.25 | 22.53 ± 2.44 | 86.26 ± 4.56 | 86.26 ± 4.56 |
| **4** | 30.24 ± 2.69 | 25.41 ± 2.44 | 68.72 ± 2.23 | 122.40 ± 5.87 |
| **5** | 33.44 ± 1.19 | 27.26 ± 1.36 | 45.60 ± 1.49 | 45.60 ± 1.49 |

[a)]Protein, 1 μM in buffer (20 mM Tris, 150 mM NaCl, 50 μM $ZnSO_4$, pH 7.4).
[b)]Active liposome composition, PC/PE/PS/dPE/Ligand (55:15:20:5:5)

compounds in monomeric form are not in complete agreement with that of under liposomal environment. Under liposomal environment compound **5** showed highest binding affinity for the C1 domains, whereas compound **3** strongly interact with the C1 domains in monomeric form. This suggests that the ligand orientation within the binding pocket is different for both in aqueous solution and under liposomal environment. Compound **5** with unsaturated fatty acid showed highest binding affinity for both the

proteins. This is in accordance with the reported binding affinity of the unsaturated DAGs to the PKC-C1 domains.[52, 53] The protein binding affinity increases with the increase in compound hydrophobicity. The molecular docking analysis and protein binding parameters shows that the kojic acid esters interact differentially with the PKC-C1 domains both in monomeric form and under liposomal environment. The binding parameters also highlight the similarity in the importance of hydrophobicity in the ligands as for other C1-domain ligands.

Some of these kojic acid esters were synthesized earlier for several intriguing pharmacological activities including, antioxidant, antitumor and others. Kojic acid esters also have several applications in food and cosmetic industries. In the present investigation, we observe that kojic acid ester interact with the lipid bilayer and influence the bilayer properties including fluidity, permeability, and phase transition temperature. The hydrophilic parts of the compounds are localized at the lipid/bilayer interface and the pharmacophores are accessible for PKC-C1 domain binding under liposomal environment. The hydroxymethyl group and carbonyl groups of pyrone ring and ester group are required for binding activity of the compounds to the C1 domains. The long-chain kojic acid ester analogues can differentially influence the in-vitro membrane interaction properties of PKCδ and PKCθ enzymes.

The higher binding affinity of the compound **5** could be due to either true selectivity of the C1 domains for ligands with unsaturated acyl chain or the effect of these ligands on the lipid bilayer organization. Higher membrane fluidity and PKC-C1 domain binding abilities was observed for the kojic acid ester with unsaturated lipid 'tail'. We hypothesize that, increase in the fluidity makes the structure of the bilayer more loosely

packed, allowing the hydrophobic surface of C1 domains to penetrate into the hydrophobic core of the lipid bilayer in a ligand-binding-dependent manner, which is essential for the PKC enzyme activation. The binding affinity differences between PKCδ- and PKCθ-C1b domains could be because of the differences in surface areas and the residues present within the binding site. The PKC activation ability of the kojic acid esters can be lower than that of phorbol ester and other natural products under similar experimental conditions. However, it is important to note that, DAG/ligand (phorbol ester) binding to the C1 domain is known to activate PKC enzymes by displacing the pseudosubstrate from the catalytic domain of the PKC enzymes. Whereas, ligand binding to the C-terminal catalytic domain generally inhibit the PKC enzyme activities. Therefore, we hypothesize that these kojic acid esters may activate PKC enzymes, due to its strong C1 domain binding capabilities. Undoubtedly further PKC activity studies are needed to fully understand the C1-domain binding mechanism of these compounds and PKC activation/inhibition properties of these ligands.

## CONCLUSION

This article illustrated that kojic acid esters interacts with lipid-bilayers and PKC-C1 domains. The results showed that strong interaction between compounds and lipid bilayers increase membrane fluidity, allow partitioning small molecules like 1-naphthol into the lipid bilayer, and decrease phase transition temperatures. The increase in fluidity of lipid bilayer structure allows the PKC-C1 domian to interact strongly with the kojic acid esters through its DAG/phorbol ester binding site. The active compounds can also compete with DAG for binding to the C1 domain under liposomal environment. The

results also indicate that both carbonyl and hydroxyl group of kojic acid esters are important for its binding to the protein. These findings suggest that, in addition to their extensive application in food, cosmetic and skin-health industries, the kojic acid esters can also be developed as research tool or lead compound in PKC-based drug development.

**Notes and references**

*Department of Chemistry, Indian Institute of Technology Guwahati, Assam 781039, India. Fax: (+) 91-361 258 2349; Tel: (+) 91-361 258 2325; E-mail: dmanna@iitg.ernet.in*

†Electronic Supplementary Information (ESI) available: [Compound characterization, fluorescence spectral data, protein binding parameters]. See DOI: 10.1039/b000000x/

‡We gratefully acknowledge CSIR (02(0090)/12/EMR-II) and DBT programme Support (No.BT/01/NE/PS/08) Govt. of India, New Delhi, India, for financial support. We are thankful to Center for Nanotechnology and CIF for instrumental support.

1. M. J. Wakelam, Biochim. *Biophys. Acta*, 1998, **1436**, 117.
2. F. Battaini and D. Mochly-Rosen, *Pharmacol. Res.*, 2007, **55**, 461.
3. G. Boije Af Gennas, V. Talman, J. Yli-Kauhaluoma, R. K. Tuominen and E. Ekokoski, *Curr. Top. Med. Chem.*, 2011, **11**, 1370.
4. Y. Nishizuka, *Science*, 1992, **258**, 607.
5. E. M. Griner and M. G. Kazanietz, *Nat. Rev. Cancer*, 2007, **7**, 281.

6. S. G. Rhee, *Annu. Rev. Biochem.*, 2001, **70**, 281.
7. F. Colon-Gonzalez and M. G. Kazanietz, *Biochim. Biophys. Acta*, 2006, **1761**, 827.
8. A. C. Newton, *Chem. Rev.*, 2001, **101**, 2353.
9. R. V. Stahelin, K. F. Kong, S. Raha, W. Tian, H. R. Melowic, K. E. Ward, D. Murray, A. Altman and W. Cho, *J. Biol. Chem.*, 2012, **287**, 30518.
10. A. C. Newton and L. M. Keranen, *Biochemistry*, 1994, **33**, 6651.
11. C. Yang and M. G. Kazanietz, *Trends Pharmacol. Sci.*, 2003, **24**, 602.
12. P. M. Blumberg, N. Kedei, N. E. Lewin, D. Yang, G. Czifra, Y. Pu, M. L. Peach and V. E. Marquez, *Curr. Drug Targets*, 2008, **9**, 641.
13. R. Zeidman, B. Lofgren, S. Pahlman and C. Larsson, *J. Cell Biol.*, 1999, **145**, 713.
14. P. J. Parker, L. Coussens, N. Totty, L. Rhee, S. Young, E. Chen, S. Stabel, M. D. Waterfield and A. Ullrich, *Science*, 1986, **233**, 853.
15. G. Manning, D. B. Whyte, R. Martinez, T. Hunter and S. Sudarsanam, *Science*, 2002, **298**, 1912.
16. J. B. Smith, L. Smith and G. R. Pettit, *Biochem. Biophys. Res. Commun.*, 1985, **132**, 939.
17. G. Boije af Gennas, V. Talman, O. Aitio, E. Ekokoski, M. Finel, R. K. Tuominen and J. Yli-Kauhaluoma, *J. Med. Chem.*, 2009, **52**, 3969.
18. V. E. Marquez and P. M. Blumberg, *Acc. Chem. Res.*, 2003, **36**, 434.
19. K. Nacro, D. M. Sigano, S. Yan, M. C. Nicklaus, L. L. Pearce, N. E. Lewin, S. H. Garfield, P. M. Blumberg and V. E. Marquez, *J. Med. Chem.*, 2001, **44**, 1892.
20. O. Raifman, S. Kolusheva, M. J. Comin, N. Kedei, N. E. Lewin, P. M. Blumberg, V. E. Marquez and R. Jelinek, *FEBS J.*, 2010, **277**, 233.
21. N. Mamidi, R. Borah, N. Sinha, C. Jana and D. Manna, *J. Phys. Chem. B*, 2012, **116**, 10684.
22. N. Mamidi, S. Gorai, R. Mukherjee and D. Manna, *Mol. Biosys.*, 2012, **8**, 1275.
23. N. Mamidi, S. Gorai, J. Sahoo and D. Manna, *Chem. Phys. Lipids*, 2012, **165**, 320.
24. T. S. Chang, *Int. J. Mol. Sci.*, 2009, **10**, 2440.
25. G. A. Burdock, M. G. Soni and I. G. Carabin, *Regul. Toxicol. Pharmacol.*, 2001, **33**, 80.
26. C. Z. Blumenthal, *Regul. Toxicol. Pharmacol*., 2004, **39**, 214.
27. R. Bentley, *Nat. Prod. Rep.*, 2006, **23**, 1046.
28. G. J. Nohynek, D. Kirkland, D. Marzin, H. Toutain, C. Leclerc-Ribaud and H. Jinnai, *Food Chem. Toxicol.*, 2004, **42**, 93.
29. M. Murou, H. Kitano, M. Fujita, M. Maeda and Y. Saruwatari, *J. Colloid Interface Sci.*, 2013, 390, 47-53.
30. H. Khandelia, B. Loubet, A. Olzynska, P. Jurkiewicz and M. Hof, *Soft Matter*, 2014, **10**, 639.
31. L. Lothstein, L. Savranskaya, C. M. Barrett, M. Israel and T. W. Sweatman, *Antican. Drugs*, 2006, **17**, 495.
32. D. Manna, N. Bhardwaj, M. S. Vora, R. V. Stahelin, H. Lu and W. Cho, *J. Biol. Chem.*, 2008, **283**, 26047.
33. D. Manna, A. Albanese, W. S. Park and W. Cho, *J. Biol. Chem.*, 2007, 282, 32093-32105.

34. N. Mamidi, S. Gorai, B. Ravi and D. Manna, *Rsc. Advan.*, 2014, 10.1039/c4ra02495h.
35. G. G. Zhang, M. G. Kazanietz, P. M. Blumberg and J. H. Hurley, Cell, 1995, **81**, 917.
36. K. Nacro, B. Bienfait, J. Lee, K. C. Han, J. H. Kang, S. Benzaria, N. E. Lewin, D. K. Bhattacharyya, P. M. Blumberg and V. E. Marquez, *J. Med. Chem.*, 2000, **43**, 921.
37. N. Brose and C. Rosenmund, *J. Cell Sci.*, 2002, **115**, 4399.
38. M. N. Hodgkin, T. R. Pettitt, A. Martin, R. H. Michell, A. J. Pemberton and M. J. Wakelam, *Trends Biochem. Sci.*, 1998, **23**, 200.
39. J. Swain, M. Mohapatra, S. R. Borkar, I. S. Aidhen and A. K. Mishra, *Phys. Chem. Chem. Phys.*, 2013, **15**, 17962.
40. E. B. Abuin, E. A. Lissi, A. Aspee, F. D. Gonzalez and J. M. Varas, *J. Colloid. Interface Sci.*, 1997, **186**, 332.
41. A. Manosroi, P. Wongtrakul, J. Manosroi, U. Midorikawa, Y. Hanyu, M. Yuasa, F. Sugawara, H. Sakai and M. Abe, *Int. J. Pharm*., 2005, **298**, 13.
42. N. Pappayee and A. K. Mishra, *Photochem. Photobiol.*, 2001, **73**, 573.
43. M. Mohapatra and A. K. Mishra, *Langmuir*, 2011, **27**, 13461.
44. M. Mohapatra and A. K. Mishra, *J. Phys. Chem. B*, 2010, **114**, 14934.
45. M. B. Lande, J. M. Donovan and M. L. Zeidel, *J. Gen. Physiol.*, 1995, **106**, 67.
46. K. E. Landgraf, C. Pilling and J. J. Falke, *Biochemistry*, 2008, **47**, 12260.
47. M. Hubert, B. J. Compton, C. M. Hayman, D. S. Larsen, G. F. Painter, T. Rades and S. Hook, *Mol. Pharm.*, 2013, **10**, 1928.
48. C. Huang, Z. Q. Wang, H. N. Lin, E. E. Brumbaugh and S. Li, *Biochim. Biophys. Acta*, 1994, **1189**, 7.
49. S. Leekumjorn and A. K. Sum, *Biochim. Biophys. Acta*, 2007, **1768**, 354.
50. J. A. Corbin, R. A. Dirkx and J. J. Falke, *Biochemistry*, 2004, **43**, 16161.
51. H. W. Huang, E. M. Goldberg and R. Zidovetzki, *Biophys. J*., 1999, **77**, 1489.
52. R. V. Stahelin, *J. Lipid Res.*, 2009, **50** Suppl, S299.
53. H. J. Mackay and C. J. Twelves, *Nat. Rev. Cancer*, 2007, **7**, 554.